AIAA 2017-1942
AIAA SciTech Forum
9 - 13 January 2017, Grapevine, Texas
AIAA Modeling and Simulation Technologies Conference

Identification and Validation of the Cessna Citation X Turbofan Modeling with Flight Tests

Paul-Alexandre Bardela and Ruxandra Mihaela Botez

Laboratory of Applied Research in Active Controls, Avionics and AeroServoElasticity LARCASE
www.larcase.etsmtl.ca
ETS, 1100 Notre Dame West, Montreal, Que., Canada, H3C-1K3

The aeronautical companies try to improve continuously their existing aircraft performances (ex: A320Néo). Thus, aircraft performances knowledge is a major issue, and it is worth developing more accurate models of aircrafts, including their engines models. The purpose of this study is to create the highest level of accuracy model possible of an airplane turbofan. The mathematical model exposed is based on a Component Level Modeling approach. This mathematical model will then be optimized using an estimation algorithm. This algorithm was performed using two approaches: a black box, and a grey box. One set of flight tests has been defined, and performed on a Cessna Citation X Research Aircraft Flight Simulator, that was designed and developed by CAE Inc., that is equipped with a D level flight dynamics toolbox. The D level is the highest fidelity rank attributed by the certification authorities for aircraft flight dynamics. The Cessna Citation X is an American long-range medium-sized business jet. It is powered by two turbofan engines AE 3007C developed by Rolls-Royce, this type of engine is a twin spool high bypass ratio turbofan.

Downloaded by IOWA STATE UNIVERSITY on January 25, 2017 | http://arc.aiaa.org | DOI: 10.2514/6.2017-1942

Nomenclature

A	=	Area
BPR	=	Bypass ratio
C	=	Velocity
C_p	=	Specific heat at constant pressure
EPR	=	Engine pressure ratio
F	=	Thrust
f	=	Fuel/air ratio by weight
FPR	=	Fan pressure ratio
H	=	Altitude
ITT	=	Turbine inlet temperature
M	=	Mach number
n	=	Polytropic efficiency
P	=	Absolute pressure
ΔP	=	Pressure loss/difference
CPR	=	Critical pressure ratio
R	=	Gas constant
T	=	Absolute temperature
ΔT	=	Temperature loss/difference
TLA	=	Throttle lever angle
W	=	Mass flow
y	=	Ratio of specific heats

[1] Master Student, ETS, LARCASE, Department of Automated Production Engineering, 1100 Notre-Dame Ouest, Montreal, Québec, CANADA, H3C1K3.
[2] Full Professor, AIAA Associate Fellow , ETS, LARCASE, Department of Automated Production Engineering, 1100 Notre-Dame Ouest, Montreal, Québec, CANADA, H3C1K3.

Copyright © 2017 by Ruxandra Mihaela Botez. Published by the American Institute of Aeronautics and Astronautics, Inc., with permission.

η	=	Efficiency
p	=	Density

Suffixes

a	=	ambient, air
b	=	combustion chamber
c	=	compressor, cold
f	=	fuel
g	=	gas
h	=	hot
j	=	nozzle
m	=	mechanical
s	=	specific

Engine references

1	=	Fan inlet
2	=	Fan outlet / High-pressure Compressor inlet
3	=	High-pressure Compressor outlet/ Combustion chamber inlet
4	=	Combustion Chamber outlet / High-pressure Turbine inlet
5	=	High-pressure Turbine outlet / Low-pressure Turbine inlet
6	=	Low-pressure Turbine inlet / Nozzle hot inlet
7	=	Hot nozzle outlet
8	=	Cold nozzle outlet

Downloaded by IOWA STATE UNIVERSITY on January 25, 2017 | http://arc.aiaa.org | DOI: 10.2514/6.2017-1942

Introduction

System identification has been widely used for model elaboration. With the technology improvements, models are constantly improve and thus present more accurate predictions. These accuracy improvements are particularly useful for the aviation industry since aircraft elaboration is strictly reglemented and constrained. All of the aircraft parameters needs to be predicted with an efficient accuracy, in all possible cases, in order to complete the certification successfully. This study focused on the thrust and fuel consumption prediction for the whole aircraft flight envelope with given altitude, Mach number and Throttle Lever Angle.

The identified model can be further derived into performance numerical dynamics[1-5] in order to optimize flight trajectory[4-15]. The Component Level Modeling (CLM) approach played a major role in engine modeling[16]. Numerous studies were performed on this method[16-23], but new tools exists now in order to model engine such as Kalman filters[24-28] and neural networks[29-31].

As its name suggest it, CLM approach is based on the modelling of each component of the engine with mechanical theoretical equations and assumptions. This approach can be done in different ways. In his study[17], Roberts modeled each component of his engine with Simulink. Nonetheless his model needs the rotation speed to determine the output of the compressor component. His solution was to determine this parameter iteratively by matching the turbine rotation speed to the compressor rotation speed since they rotate at the same speed. In this case the fuel flow is considered as an input. The thrust output is predicted for a given altitude, Mach number and fuel flow.

Others studies uses the CLM approach in order to predict the components efficiencies deterioration and their impact on the thrust output of the engine[32]. This kind of studies can also be derived into fault diagnosis studies[33]. These kinds of studies elaborate models in order to predict engine issues such as fooling for example.

The purpose of this study is to elaborate a model predicting thrust and fuel flow outputs with given altitudes, Mach number and Throttle Lever Angle as accurate as possible. This model is based on a Component Level Modeling adapted to the engine studied using flight tests data.

One set of flight tests have been defined, and executed on a Cessna Citation X Research Aircraft Flight Simulator, that was designed and developed by CAE Inc., and equipped with a D level flight dynamics toolbox. The D level is the highest fidelity rank attributed by the certification authorities for flight dynamics.

Figure1. Cessna Citation X Level D Flight Simulator

I. System identification

A. Method

The basic principle of "system identification" is to obtain a system using inputs and outputs data. One can refer to various references in this area[34-44] . The procedure is described on the following figure:

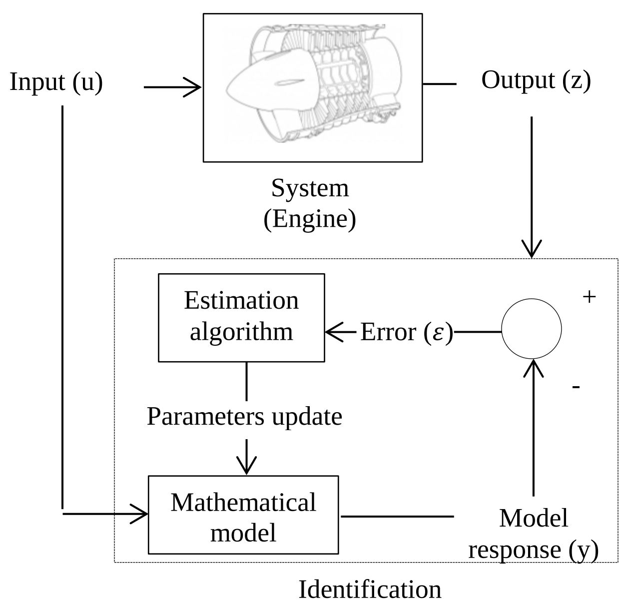

Figure 2. System identification process apply to engine

For this study, u is the Mach number M , the altitude H and the Throttle lever angle TLA measured with the simulator; z represents the fuel flow Wf and the net thrust Fn; y represent the fuel flow and net thrust calculated with the mathematical model; ε represent the difference between the measured outputs z and the model response y.

Downloaded by IOWA STATE UNIVERSITY on January 25, 2017 | http://arc.aiaa.org | DOI: 10.2514/6.2017-1942

Downloaded by IOWA STATE UNIVERSITY on January 25, 2017 | http://arc.aiaa.org | DOI: 10.2514/6.2017-1942

B. Estimation algorithm

As described in Figure 2, an estimation algorithm is needed in order to fit the mathematical model to the experimental data. The parameters of the mathematical model θ are updated in order to minimize the cost function $J(\theta)$. In this study, the Least Square (LS) method is used, and the cost function is expressed as function of the error between the model response and the experimental data ε .

$$J(\theta) = \sum_{k=1}^{N} \varepsilon(\mathrm{k})^2 = \varepsilon^t \varepsilon \tag{1}$$

The LS method was largely used in order to approximate non-linear functions. This LS method was applied in this paper to polynomial functions. Since these functions are orthogonal, the Levenberg-Marquardt algorithm[45] may provide an accurate solution in order to determine their coefficients of the polynomial function. Yet this method consider a maximal number of two inputs and our outputs depends of three inputs (*M*, *H* and *TLA*). The algorithm can't be directly applied. In order to avoid this problem the choice was to fix the *TLA* values. Then a polynomial function, Fn_{HM}, was found for each *TLA* values depending on *H* and *M*.

$$Fn_{HM}(H, M) = \sum_{i=0}^{n} \sum_{j=0}^{m} p_{ij} M^i H^j \tag{2}$$

A polynomial function, depending on the *TLA*, was obtained with the same algorithm to fit to the coefficients p_{ij} found previously.

$$p_{ij}(TLA) = \sum_{k=0}^{l} p_k\, TLA^k \tag{3}$$

With the method exposed, two polynomial functions were obtained, that depend on the three inputs parameters; the net trust *Fn* and the fuel flow Wf are obtained with the following equations:

$$Fn_{total}(H, M, TLA) = \sum_{i=0}^{n} \sum_{j=0}^{m} p_{ij}(TLA) M^i H^j \tag{4}$$

$$W_{total}(H, M, TLA) = \sum_{i=0}^{n} \sum_{j=0}^{m} q_{ij}(TLA) M^i H^j \tag{5}$$

where $p_{ij}(TLA) = \sum_{k=0}^{l} p_k\, TLA^k$ and $q_{ij}(TLA) = \sum_{k=0}^{l} q_k\, TLA^k$; p_k and q_k are the coefficients of the polynomial functions, and *n,m, l* are the degrees of the polynomial functions.

No theoretical functions are used to determine this model; this approach exposed here will be called "Black box" in the rest of this paper.

C. Flight tests distribution

In order to identify the turbofan model, a number of 25 flight tests were executed on the Level D flight test simulator, and dispatched over its flight envelope. The level D ensures us a fine accuracy of the simulator acquired data as is the highest level of certification for the aircraft flight dynamics. These flight tests were performed for TLA and altitude fixed, while the aircraft accelerated. The TLA varied from 42 % to 100 % and the altitude varied from 5,000 ft, to 45,000 ft. These ranges were chosen because most airplanes fly between these two altitudes and TLAs.

For low TLA values, less than 42%, most airplanes cannot fly at a fixed altitude. It was noticed that during the flight test, the acceleration is not the same according to the altitude: it is easier to accelerate at low altitude, thus fewer points are obtained than at high altitude because the max speed is reached quicker. Thus the model does not predict accurately low altitude flight tests because the meshing of the flight envelope is unbalanced. To solve this problem, the identification flight test data are extrapolated in order to enlarge the number of data points to 500 points in order to balance the meshing. The final meshing is presented on the following Table 1. The identification flight tests cases are presented in "red", and the validation flight tests are shown in "blue".

Downloaded by IOWA STATE UNIVERSITY on January 25, 2017 | http://arc.aiaa.org | DOI: 10.2514/6.2017-1942

TLA Altitude	35	37.5	40	42.5	45	47.5	50	52.5	55	57.5	60	62.5	65
5000	X	X	X	X	X	X	X	X	X	X	X	X	X
10000	X	X	X	X	X	X	X	X	X	X	X	X	X
15000	X	X	X	X	X	X	X	X	X	X	X	X	X
20000	X	X	X	X	X	X	X	X	X	X	X	X	X
25000	X	X	X	X	X	X	X	X	X	X	X	X	X
30000	X	X	X	X	X	X	X	X	X	X	X	X	X
35000	X	X	X	X	X	X	X	X	X	X	X	X	X
40000	X	X	X	X	X	X	X	X	X	X	X	X	X
45000	X	X	X	X	X	X	X	X	X	X	X	X	X

Table 1. Identification (25) and validation (90) flight tests distribution

These cases are shown in Table 1 for different TLAs and altitudes.

II. System modeling

D. Thrust modeling

The principle of CLM method is to consider each of the turbofan components, and to use an independent submodule for each component (of the turbofan). Thus, performance map is used for the compressor model, for example. The combination of all these models leads to the final model.

The main issue of the CLM method is obtaining the compressor and turbine performances maps. These maps allow the user to predict the different pressure ratios and the mass flow exiting for each rotational speed of the rotor. But these maps cannot be obtained on the simulator because of the fact that some values of these variables are not given by the research simulator code such as the exiting mass flow. Nonetheless, this simulator provides the Fan Pressure Ratio (*FPR*), the Engine Pressure Ratio (*EPR*), and the Turbine Inlet Temperature (*ITT*). Using these three parameters as inputs, it is possible to obtain the thrust and the fuel flow using the classical thermodynamics equations and the correct assumptions. These equations are given in the Appendix 1 of this paper.

Those three parameters are not part of the system inputs specified Section I)A). To replace the compressor/turbine performances maps, polynomial functions of those three parameters (*FPR*, *EPR*, *ITT*) are obtained using the black box method described in Section I)B). The inputs are unchanged (*M*, *H*, *TLA*) but the outputs are *FPR*, *EPR*, and *ITT*, and thus three polynomial functions are obtained, and expressed in equations (6) - (8).

$$FPR(H,M,TLA) = \sum_{i=0}^{n}\sum_{j=0}^{m} r_{ij}(TLA)M^iH^j \tag{6}$$

$$EPR(H,M,TLA) = \sum_{i=0}^{n}\sum_{j=0}^{m} r'_{ij}(TLA)M^iH^j \tag{7}$$

$$ITT(H,M,TLA) = \sum_{i=0}^{n}\sum_{j=0}^{m} r''(TLA)M^iH^j \tag{8}$$

In fact, a smaller number of flight tests are necessary to identify and validate *FPR*, *EPR and ITT* with a fine accuracy than the number of flight tests needed to identify and validate the fuel flow and the thrust.

Downloaded by IOWA STATE UNIVERSITY on January 25, 2017 | http://arc.aiaa.org | DOI: 10.2514/6.2017-1942

Yet, to use the thermodynamic system shown in Appendix 1, some constant values are needed. Firstly, polytrophic, compression, fan and expansion efficiencies will be determined. For easier modeling purpose, polytrophic, compression, fan and expansion efficiencies are supposed to be equal in this research.

$$\eta_p = \eta_f = \eta_c \tag{9}$$

To find the polytropic efficiency η_p, the first equation from the thermodynamic system is used:

$$T_2 = T_1 . FPR^{\frac{\gamma_a}{\eta_p \cdot (\gamma_a - 1)}} \tag{10}$$

In the identification flights tests, the temperature at the exit of fan T_2 was also measured. Then, η_p was identified in equation (11) using a reformulation of equation (10):

$$\eta_p = \frac{\gamma_a - 1}{\gamma_a} / \log \frac{T_2/T_1}{FPR} \tag{11}$$

We could choose a constant coefficient of efficiency, η_p, value but we decided to suppose that this efficiency depends on M as a fifth order polynomial function to increase its precision:

$$\eta_p\,(FPR) = \sum_{i=1}^{5} s_i \,.\, FPR^i \tag{12}$$

With this expression of the compressor efficiency, the temperature at the exit of fan T_2 is found accurately using equation (10).

Then thermodynamically constant C_p and y have to be also determined. The assumption is that these constants only depend on the ambient air temperature. A table of different C_p and y determined at various temperatures from 175 K to 1900 K were to obtained by use of a 6th order polynomial function of C_p and y :

$$Cp\,(T) = \sum_{i=1}^{6} t_i \,.\, T^i \tag{13}$$

$$y\,(T) = \sum_{i=1}^{6} t'_i \,.\, T^i \tag{14}$$

There are four constants needed to be determined, the Bypass Ratio *BPR*, the propelling nozzle efficiency η_j, the mechanical efficiency η_m, and the combustion chamber pressure loss ΔP_b.

Unlike the constants previously determined (Cp, y, η_p), we cannot determine them directly because the simulator does not measure all the variables of the equations within these variables appears. The Levenberg-Marquart algorithm was chosen in order to determine these constants. By using this algorithm, the different constants vary in a fixed range starting from a fixed point.

In the literature[23], approximated values of these constants are known for a twin-spool turbofan. A range is then fixed around these possible values. The thrust is expressed with the different equations from the Appendix 1 and the algorithm finds the best values of the four constants in order to fit the thrust function with the actual thrust value measured using the simulator. The detailed Levenberg-Marquart algorithm can be found in the Appendix 2.

Finally all the unknown variables are identified, so that the thermodynamically system can be obtained. Yet the generic model is not very accurate model. As explained in the Section I.B, an estimation algorithm is used in order to improve the model. In our case, a fifth order polynomial function depending on *M* and *FPR* gave the best results than other combination such as *H* and *TLA* for example:

$$F_{total}\,(M, H, TLA) = F_{CLM} \cdot \sum_{i=0}^{n} \sum_{j=0}^{m} v_{ijk} M^i FPR^j \tag{15}$$

Downloaded by IOWA STATE UNIVERSITY on January 25, 2017 | http://arc.aiaa.org | DOI: 10.2514/6.2017-1942

E. Fuel flow modeling

Fuel Flow (W_f) is much more difficult to predict than the thrust. This difficulty might be due to the fact that the fuel flow is controlled by the computer integrated in the aircraft (FADEC). For example, the fuel flow is controlled in order to keep reasonable the combustor outlet temperature not too high. In fact a too high temperature might damage the turbine blade positioned next to the combustor. According to Saravanamuttoo [23] the fuel flow can be expressed with equation (16):

$$W_f = f.\frac{W_a}{BPR+1} \tag{16}$$

where W_a is the inlet air mass flow, BPR is the bypass ratio, and f is the fuel ratio.

The fuel ratio is obtained in the same way in which the polytrophic efficiency is obtained. The fuel flow W_f and the air flow W_a are measured using the simulator, and the best fit is found for f by using Matlab fitting tools. We suppose that f only depends on the FPR and the TLA, and that a 5th order polynomial function is obtained:

$$f\,(FPR, TLA) = \sum_{i=0}^{n}\sum_{j=0}^{m} u_{ij} FPR^{i} TLA \tag{17}$$

Finally, the fuel flow model can be synthetized with the following equation:

$$W_{f_{total}}(H, M, TLA) = f(FPR, TLA).\frac{W_a}{B+1} \tag{18}$$

III. Validation of Results

The validation process is necessary in order to evaluate the accuracy of the identified model. The validation criteria from the FAA were used. A validation success is obtained if the thrust and the fuel flow are predicted within 5% error. The model identified in the previous section using the 25 identification flight tests is applied on a new set of 90 validation flight tests. The results are presented in the following Tables 2 and 3:

	Identification success (%)	**Validation success (%)**	**Mean absolute relative error (%)**
Estimation algorithm only	100	81.72	2,70
Thermodynamic system optimized	100	96.33	1.62

Table 2. Thrust results obtained by 25 identification flight tests and 90 validation flight tests

	Identification success (%)	**Validation success (%)**	**Mean absolute relative error (%)**
Estimation algorithm only	100	67.90	4.84
Thermodynamic system optimized	100	64.90	5.23

Table 3. Fuel flow results obtained by 25 identification flight tests and 90 validation flight tests

Downloaded by IOWA STATE UNIVERSITY on January 25, 2017 | http://arc.aiaa.org | DOI: 10.2514/6.2017-1942

IV. Conclusion

In this paper, a Cessna Citation X engine model was identified using a minimum set of flight tests. This model predicts the thrust and fuel flow outputs for given altitudes, Mach numbers and *TLA* inputs. A two-step approach was performed because a generic model was extracted from the literature and adapted to the studied case.

This model was therefore optimized based on the LS method, by using the Levenberg-Marquardt algorithm. Two different models were compared:

1) a "black box" model that used only the estimation algorithm, and
2) a "grey box" model combined the generic model with the estimation algorithm.

The results have shown that the first estimation algorithm alone gave only 81.7 % validation success. The "grey box" model approaches gave 96.33 % validation success for thrust outputs. The generic model was determined in order to represent each component of the engine, yet, since all parameters were interrelated, it remained a difficult task to model each component.

All components gave relative errors, thus the global error quickly increased. A more accurate approach in future for the determination of each component might give more accurate results. For example, it was noticed that if the *FPR* was used as an input, the validation success was of 100 % for the thrust prediction. Yet, about the fuel flow prediction, the results were less accurate than the results obtained for the thrust (64 % validation success in the grey box approach). It seems logical because the mathematical model was less elaborated than the mathematical thrust model. The Black Box model gave better more accurate results (67 % validation success) than "grey box" approach for the fuel flow prediction. These results showed that the fuel flow generic model was not adapted for the black box model. A more elaborate generic model would certainly lead to more accurate results.

Other estimation algorithm might be more adapted to solve this problem such as the Thrust-Region and Particle Swarm Optimization. These algorithms will be developed in future studies. Different generic model might provide more accurate results such as "Mattingly" for example.

Appendix 1. The thermodynamics equations system[23]

Nomenclature

A	=	Area
BPR	=	Bypass ratio
C	=	Velocity
C_p	=	Specific heat at constant pressure
EPR	=	Engine pressure ratio
F	=	Thrust
f	=	Fuel/air ratio by weight
FPR	=	Fan pressure ratio
H	=	Altitude
ITT	=	Turbine inlet temperature
M	=	Mach number
n	=	Polytropic efficiency
P	=	Absolute pressure
ΔP	=	Pressure loss/difference
CPR	=	Critical pressure ratio
R	=	Gas constant
T	=	Absolute temperature
ΔT	=	Temperature loss/difference
TLA	=	Throttle lever angle
W	=	Mass flow
y	=	Ratio of specific heats
η	=	Efficiency
p	=	Density

Suffixes

a	=	ambient, air
b	=	combustion chamber
c	=	compressor, cold
f	=	fuel
g	=	gas
h	=	hot
j	=	nozzle
m	=	mechanical
s	=	specific

Engine references

1	=	Fan inlet
2	=	Fan outlet / High-pressure Compressor inlet
3	=	High-pressure Compressor outlet/ Combustion chamber inlet
4	=	Combustion Chamber outlet / High-pressure Turbine inlet
5	=	High-pressure Turbine outlet / Low-pressure Turbine inlet
6	=	Low-pressure Turbine inlet / Nozzle hot inlet
7	=	Hot nozzle outlet
8	=	Cold nozzle outlet

Downloaded by IOWA STATE UNIVERSITY on January 25, 2017 | http://arc.aiaa.org | DOI: 10.2514/6.2017-1942

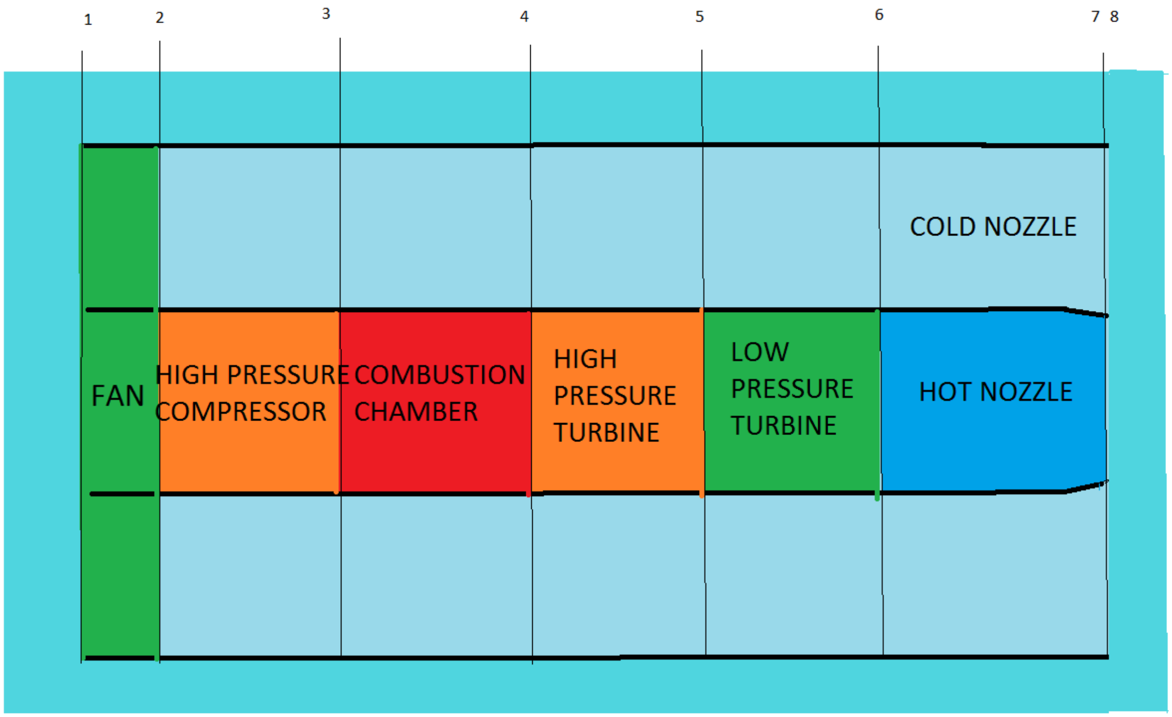

Figure 3 .Turbofan schemes with the engine references

The temperature at the outlet of the fan T_2 and at the outlet of the compressor T_3 are calculated using the isentropic equations with the fan efficiency η_f, the compressor efficiency η_c, the adiabatic coefficient at air inlet temperature γ_a, the inlet temperature T_1 the Fan Pressure Ratio (FPR) and the Engine Pressure Ratio (EPR) :

$$T_2 = T_1 . FPR^{\frac{\gamma_a}{\eta_f \cdot (\gamma_a - 1)}} \tag{19}$$

$$T_3 = T_2 . \left(\frac{EPR}{FPR}\right)^{\eta_c \frac{\gamma_a}{\gamma_a - 1}} \tag{20}$$

Then the cold nozzle temperature drop, ΔT_{28}, is calculated:

$$\Delta T_{28} = T_2 - T_8 = \eta_J . T_2 . [1 - ({}^{1}/_{FPR})^{\frac{\gamma_a}{\eta_c \cdot (\gamma_a - 1)}}] \tag{21}$$

The cold critical pressure ratio CPR_C is evaluated in order to know if the cold part of the nozzle is chocked.

$$CPR_C = \left[\frac{\eta_J}{\left(\eta_J - {}^{(\gamma_a - 1)}/_{(\gamma_a + 1)}\right)}\right]^{\frac{\gamma_a}{\eta_c \cdot (\gamma_a - 1)}} \tag{22}$$

If $FPR < CPR_c$ then the cold nozzle is not chocked and the gas is fully extended: $P_8 = P_a$

$$C_8 = \left[2 . C_{pa} . (T_2 - T_8)\right]^{0.5} \tag{23}$$

Downloaded by IOWA STATE UNIVERSITY on January 25, 2017 | http://arc.aiaa.org | DOI: 10.2514/6.2017-1942

The cold thrust F_c depending on the inlet air mass flow W_a and the Bypass Ratio BPR is given by:

$$F_c = \frac{W_a.BPR}{BPR+1}.C_8 \tag{24}$$

If the cold nozzle is chocked, then:

$$P_8 = \frac{P_a}{PR_c} \tag{25}$$

$$F_c = \frac{W_a.B}{B+1}.C_8 + A_8(P_8 - P_a) \tag{26}$$

The work needed for the high-pressure shaft produced by the turbine gives the following equation:

$$ITT - T_5 = \frac{Cp_a}{\eta_m.Cp_g}(T_3 - T_2) \tag{27}$$

The work needed for the low-pressure shaft produced by the turbine gives the following equation:

$$T_5 - T_6 = (B+1).\frac{Cp_a}{\eta_m.Cp_g}(T_2 - T_1) \tag{28}$$

The pressure drop ΔP_b from the combustion is supposed constant, the burner exit pressure is then expressed with the inlet pressure, and the EPR:

$$P_4 = EPR.P_1 - \Delta P_b \tag{29}$$

The pressure at the outlet of the high pressure turbine P_5 and at the outlet of the pressure of the low pressure turbine P_6 are calculated using the isentropic equation with the turbine efficiency η_t:

$$P_5 = P_4.({T_5}/{ITT})^{\eta_t\frac{\gamma_g}{\gamma_g-1}} \tag{30}$$

$$P_6 = P_5.({T_6}/{T_5})^{\eta_t\frac{\gamma_g}{\gamma_g-1}} \tag{31}$$

Then, the hot nozzle temperature drop is calculated, in the same way as equation (21):

$$T_7 = T_6.\{1 - \eta_J.[1 - ({P_1}/{P_6})^{\eta_t\frac{\gamma_g}{\gamma_g-1}}]\} \tag{32}$$

$$C_7 = \left[2.C_{pg}.(T_7 - T_6)\right]^{0.5} \tag{33}$$

The hot critical pressure ratio CPR_h is evaluated in order to know if the hot nozzle is chocked.

$$CPR_h = \left[\frac{\eta_J}{\left(\eta_J - {(\gamma_g - 1)}/{(\gamma_g + 1)}\right)}\right]^{\eta_t\frac{\gamma_g}{\gamma_g-1}} \tag{34}$$

If $\frac{P_6}{P_1} < CPR_h$, then the hot nozzle is not chocked and the gas is fully extended: $P_7 = P_a$

The hot thrust F_h is given by:

$$F_h = \frac{W_a.}{B+1}.C_7 \tag{35}$$

Downloaded by IOWA STATE UNIVERSITY on January 25, 2017 | http://arc.aiaa.org | DOI: 10.2514/6.2017-1942

If not, the hot nozzle is chocked and then:

$$P_7 = \frac{P_6}{PR_h} \tag{36}$$

$$F_h = \frac{W_a}{B+1}.C_8 + A_8(P_7 - P_a) \tag{37}$$

The total thrust net thrust F_n is:

$$F_n = F_c + F_h - W_a.C_a \tag{38}$$

The fuel flow W_f is calculated as follows:

$$W_f = f.\frac{W_a}{B+1} \tag{39}$$

Where f is the ratio of fuel on air in the combustion chamber.

Downloaded by IOWA STATE UNIVERSITY on January 25, 2017 | http://arc.aiaa.org | DOI: 10.2514/6.2017-1942

Downloaded by IOWA STATE UNIVERSITY on January 25, 2017 | http://arc.aiaa.org | DOI: 10.2514/6.2017-1942

Appendix 2. The Levenberg-Marquart algorithm[34,35]

The purpose of this algorithm is to solve non-linear squares problems by finding a least square fitting between output data and the output of the thrust function F, particularly in this paper. This fitting is find here by adjusting the Bypass Ratio BPR, the nozzle efficiency η_j, the mechanical efficiency η_m, and the pressure drop in the burner ΔP_b.

$$\varepsilon(x_0) = \sum_{n=1}^{m} \left(y_i - F(x_i, x_0)\right)^2 \tag{40}$$

ε: Error to minimize
y_i: Output data (thrust)
x_i: Input data (Altitude, Mach number, Throttle Lever Angle)
x_0: Starting constant vector $\left[BPR_0, \eta_{j_0}, \eta_{m_0}, \Delta P_{b_0}\right]$
q: Difference between x_0 and the next value of x_0

The solution is based on the following assumption:

$$F(x_i, x_0 + q) \cong F(x_i, x_0) + J_i . q \tag{41}$$

J_i is the Jacobian of the thrust function F, derived with respect to the vector x_0.

$$J_i = \frac{dF(x_i, x_0)}{dx_0} \tag{42}$$

Then, equation (40) becomes

$$\varepsilon(x_0 + q) \cong \sum_{n=1}^{m} (y_i - F(x_i, x_0) - J_i . q)^2 \tag{43}$$

Then, in the vector notation:

$$\varepsilon(x_0 + q) \cong \|y - F(x_0) - J.q\|^2$$

$$\varepsilon(x_0 + q) = (y - F(x_0) - J.q)^T (y - F(x_0) - J.q) \tag{44}$$

$$\varepsilon(x_0 + q) = \left(y - F(x_0)\right)^T \left(y - F(x_0)\right) - 2\left(y - F(x_0)\right)^T . J.q + q^T . J^T . J.q$$

By deriving $\varepsilon(x_0 + q)$ from equation (44) by q and then by rearranging the equation, we obtain:

$$q = J^T . (y - F(x_0)) . (J^T . J)^{-1} \tag{45}$$

In this research, we use a “damped version” of the algorithm by adding the damping parameter λ in equation (45):

$$q = J^T . (y - F(x_0)) . (J^T . J + \lambda . I)^{-1} \tag{46}$$

In this process, x_0 is replaced by $x_0 + q$ at every iteration until the desired convergence is reached. The precision criteria is 10^{-3}.

Downloaded by IOWA STATE UNIVERSITY on January 25, 2017 | http://arc.aiaa.org | DOI: 10.2514/6.2017-1942

Acknowledgments

This study was performed at the Laboratory of Applied Research in Active Controls, Avionics and AeroServoElasticity Research (LARCASE). The Research Aircraft Flight Simulator was obtained by Dr Ruxandra Botez, Full Professor, thanks to the research grants that were approved by the Canadian Foundation of Innovation (CFI), Ministère du Développement Économique, de l'Innovation et de l'Exportation (MDEIE) and the contribution of CAE Inc. Thanks are dues to CAE Inc. team led by Mr Ken Dustin, and to Mr. Oscar Carranza Moyao for their support in the development of the Research Aircraft Flight Simulator at the LARCASE laboratory. Thanks are also dues to Mrs Odette Lacasse at ETS for her support.

References

1. Murrieta Mendoza, A., Demange, S., George, F., and Botez, R. "Performance Database Creation Using a Flight D Simulator For Cessna Citation X Aircraft in Cruise Regime," *The 34th IASTED International Conference on Modelling, Identification, and Control (MIC2015)*. 2015.
2. Murrieta-Mendoza, A., Demange, S., George, F., and Botez, R. "Performance DataBase creation using a level D simulator for Cessna Citation X aircraft in cruise regime," *IASTED Modeling, Identification and Control Conference, Innsbruck, Austria*. 2015.
3. Patrón, R. S. F., Berrou, Y., and Botez, R. M. "New methods of optimization of the flight profiles for performance database-modeled aircraft," *Proceedings of the Institution of Mechanical Engineers, Part G: Journal of Aerospace Engineering* Vol. 229, No. 10, 2015, pp. 1853-1867.
4. Murrieta-Mendoza, A., and Botez, R. "Method to Calculate Aircraft VNAV Trajectory cost Using a Performance Database," *ASME 2014 International Mechanical Engineering Congress and Exposition*. American Society of Mechanical Engineers, 2014, pp. V001T01A053-V001T01A053.
5. Murrieta-Mendoza, A., and Botez, R. M. "Methodology for Vertical-Navigation Flight-Trajectory Cost Calculation Using a Performance Database," *Journal of Aerospace Information Systems* Vol. 12, No. 8, 2015, pp. 519-532.
6. Beulze, B., Dancila, B., Botez, R., Bottollier-Lemallaz, S., and Herda, S. "Presentation of three methods results comparison for Vertical Navigation VNAV trajectory optimization for the Flight Management System FMS," *15th AIAA Aviation Technology, Integration, and Operations Conference*. 2015, p. 2597.
7. Dancila, B. D., and Botez, R. M. "Construction of an aircraft's VNAV flight envelope for in-FMS flight trajectory computation and optimization," *14th AIAA Aviation Technology, Integration, and Operations Conference*. 2014, p. 2291.
8. Gautier, M. M., Dancila, R., and Botez, R. M. "Optimization of the Cruise Regime of Flight Airplane Trajectory using Deterministic Algorithms," *15th AIAA Aviation Technology, Integration, and Operations Conference*. 2015, p. 3179.
9. Liv, A., Dancila, R. I., and Botez, R. M. "Trajectory optimization algorithm for a constant altitude cruise flight with a required time of arrival constraints," *15th AIAA Aviation Technology, Integration, and Operations Conference*. 2015, p. 2282.
10. Mendoza, A. M., Beuze, B., Ternisien, L., and Botez, R. "Branch & Bound Based Algorithm For Aircraft VNAV Profile Reference Trajectory Optimization," 2015.
11. Mendoza, A. M., and Botez, R. "Vertical navigation trajectory optimization algorithm for a commercial aircraft," *AIAA/3AF Aircraft Noise and Emissions Reduction Symposium*. 2014.
12. Murrieta-Mendoza, A., Botez, R., and Labour, D. "Vertical navigation trajectory optimization algorithm for the lockheed l-1011," *AIAA Aicraft Noise and Emissions Reduction Symposium, Atlanta, GA*. 2014.
13. Patrón, R. S. F., Berrou, Y., and Botez, R. M. "Climb, Cruise and Descent 3D Trajectory Optimization Algorithm for a Flight Management System," *AIAA Aviation 2014*, 2014, pp. 16-20.
14. Patrón, R. S. F., and Botez, R. M. "Flight trajectory optimization through genetic algorithms coupling vertical and lateral profiles," *ASME 2014 International Mechanical Engineering Congress and Exposition*. American Society of Mechanical Engineers, 2014, pp. V001T01A048-V001T01A048.
15. Sidibé, S., and Botez, R. "Trajectory optimization of FMS-CMA 9000 by dynamic programming," *ASI AÉRO 2013 conference, 60th Aeronautics Conference and AGM, Toronto, Canada*. 2013.
16. Suraweera, J. K. "Off-Design Performance Prediction of Gas Turbines without the use of Compressor or Turbine Characteristics." Carleton University Ottawa, 2011.
17. Roberts, R. A., and Eastbourn, S. M. "Modeling techniques for a computational efficient dynamic turbofan engine model," *International Journal of Aerospace Engineering* Vol. 2014, 2014.

18. Bazazzade, M., Shahriari, A., and Badihi, H. "Improved turbine engine hierarchical modeling and simulation based on engine fuel control system," *Journal of Aerospace Science & Technology [JAST], ISSN*, 2009, pp. 1735-2134.
19. Szuch, J. R., Krosel, S. M., and Bruton, W. M. "An automated procedure for developing hybrid computer simulations of turbofan engines," *Proceedings of the 14th annual symposium on Simulation*. IEEE Press, 1981, pp. 79-94.
20. Cai, N., Li, H. W., Li, M., and Ye, B. "Modeling and Simulation of Turbofan Engine Based on Modularized Subassembly," *Applied Mechanics and Materials*. Vol. 599, Trans Tech Publ, 2014, pp. 353-357.
21. Yao, H. T., Wang, X., and Kong, X. X. "A Real-Time Transient Model of CF6 Turbofan Engine," *Applied Mechanics and Materials*. Vol. 241, Trans Tech Publ, 2013, pp. 1573-1585.
22. Martin, S., Wallace, I., and Bates, D. G. "Development and validation of a civil aircraft engine simulation model for advanced controller design," *Journal of Engineering for Gas Turbines and Power* Vol. 130, No. 5, 2008, p. 051601.
23. Saravanamuttoo, H. I. H., Rogers, G. F. C., and Cohen, H. *Gas turbine theory*: Pearson Education, 2001.
24. Sugiyama, N. "Derivation of system matrices from nonlinear dynamic simulation of jet engines," *Journal of Guidance, Control, and Dynamics* Vol. 17, No. 6, 1994, pp. 1320-1326.
25. Sugiyama, N. "On Line System Identification of Jet Engine," *AIAA, ASME, SAE, and ASEE, Joint Propulsion Conference and Exhibit, 32 nd, Lake Buena Vista, FL*. 1996.
26. Sugiyama, N. "System identification of jet engines," *ASME 1998 International Gas Turbine and Aeroengine Congress and Exhibition*. American Society of Mechanical Engineers, 1998, pp. V005T15A007-V005T15A007.
27. Luppold, R., Roman, J., Gallops, G., and Kerr, L. "Estimating in-flight engine performance variations using Kalman filter concepts," *AIAA, ASME, SAE, and ASEE, Joint Propulsion Conference, 25 th, Monterey, CA*. 1989, p. 1989.
28. Kobayashi, T., Simon, D. L., and Litt, J. S. "Application of a constant gain extended Kalman filter for in-flight estimation of aircraft engine performance parameters," *ASME Turbo Expo 2005: Power for Land, Sea, and Air*. American Society of Mechanical Engineers, 2005, pp. 617-628.
29. Kobayashi, T., and Simon, D. L. "Hybrid neural-network genetic-algorithm technique for aircraft engine performance diagnostics," *Journal of Propulsion and Power* Vol. 21, No. 4, 2005, pp. 751-758.
30. Tayarani-Bathaie, S. S., Vanini, Z. S., and Khorasani, K. "Dynamic neural network-based fault diagnosis of gas turbine engines," *Neurocomputing* Vol. 125, 2014, pp. 153-165.
31. Mathioudakis, K., and Romessis, C. "Probabilistic neural networks for validation of on-board jet engine data," *Proceedings of the Institution of Mechanical Engineers, Part G: Journal of Aerospace Engineering* Vol. 218, No. 1, 2004, pp. 59-72.
32. Ogaji, S., Sampath, S., Singh, R., and Probert, S. "Parameter selection for diagnosing a gas-turbine's performance-deterioration," *Applied Energy* Vol. 73, No. 1, 2002, pp. 25-46.
33. Baig, M. F., and Sayeed, N. "Model-based reasoning for fault diagnosis of twin-spool turbofans," *Proceedings of the Institution of Mechanical Engineers, Part G: Journal of Aerospace Engineering* Vol. 212, No. 2, 1998, pp. 109-116.
34. Jategaonkar, R. *Flight vehicle system identification: a time domain methodology*: AIAA, Reston, VA, USA, 2006.
35. Klein, V., and Morelli, E. A. *Aircraft system identification: theory and practice*: American Institute of Aeronautics and Astronautics Reston, Va, USA, 2006.
36. Beaulieu, M., Mota, S. D. J., and Botez, R. "Identification of structural surfaces' positions on an F/A-18 using the subspace identification method from flight flutter tests," *Proceedings of the Institution of Mechanical Engineers, Part G: Journal of Aerospace Engineering* Vol. 221, No. 5, 2007, pp. 719-731.
37. Boëly, N., and Botez, R. M. "New approach for the identification and validation of a nonlinear F/A-18 model by use of neural networks," *IEEE Transactions on Neural Networks* Vol. 21, No. 11, 2010, pp. 1759-1765.
38. Boely, N., Botez, R. M., and Kouba, G. "Identification of a non-linear F/A-18 model by the use of fuzzy logic and neural network methods," *Proceedings of the Institution of Mechanical Engineers, Part G: Journal of Aerospace Engineering* Vol. 225, No. 5, 2011, pp. 559-574.
39. De Jesus-Mota, S., Nadeau Beaulieu, M., and Botez, R. "Identification of a MIMO state space model of an F/A-18 aircraft using a subspace method," *Aeronautical Journal* Vol. 113, No. 1141, 2009, p. 183.
40. Ghazi, G., Botez, R., and Achigui, J. M. "Cessna Citation X Engine Model Identification from Flight Tests," *SAE International Journal of Aerospace* Vol. 8, No. 2015-01-2390, 2015, pp. 203-213.
41. Hamel, C., Sassi, A., Botez, R., and Dartigues, C. "Cessna Citation X aircraft global model identification from flight tests," *SAE International Journal of Aerospace* Vol. 6, No. 2013-01-2094, 2013, pp. 106-114.

Downloaded by IOWA STATE UNIVERSITY on January 25, 2017 | http://arc.aiaa.org | DOI: 10.2514/6.2017-1942

42. Kouba, G., Botez, R. M., and Boely, N. "Fuzzy logic method use in F/A-18 aircraft model identification," *Journal of aircraft* Vol. 47, No. 1, 2010, pp. 10-17.
43. Mota, S. D. J., and Botez, R. "New helicopter model identification method based on flight test data," *Aeronautical Journal* Vol. 115, No. 1167, 2011, p. 295.
44. Nadeau Beaulieu, M., and Botez, R. "Simulation and prediction of the helicopter main rotor, tail rotor and engine parameters by using the subspace system identification method," *J Aerospace Eng* Vol. 222, 2008, pp. 817-834.
45. Marquardt, D. W. "An algorithm for least-squares estimation of nonlinear parameters," *Journal of the society for Industrial and Applied Mathematics* Vol. 11, No. 2, 1963, pp. 431-441.

Downloaded by IOWA STATE UNIVERSITY on January 25, 2017 | http://arc.aiaa.org | DOI: 10.2514/6.2017-1942